JACS
JOURNAL OF THE AMERICAN CHEMICAL SOCIETY

Open Access
This article is licensed under CC-BY 4.0

pubs.acs.org/JACS
Article

Excited-State Branching in Optovin: Resolving the Photophysics of a Gene-Free Optopharmacological Tool

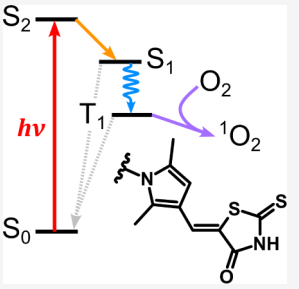
Jonathan Q. Brouwer, Alex J. Cook, Eleanor K. Ashworth, Anam Fatima, Khalid M. Siddiqui, Isabelle Chambrier, Andrew N. Cammidge, Pratip Chakraborty, Wesley R. Browne, Stephen R. Meech, and James N. Bull*

Cite This: https://doi.org/10.1021/jacs.6c13271

Read Online

ACCESS | Metrics & More | Article Recommendations | Supporting Information

ABSTRACT: Optovin is a small, light-activated molecule that enables optical control of TRPA1 ion channels without genetic modification, making it a landmark tool in optopharmacology. However, the excited-state pathways initiated by photoexcitation, and how these may relate to optovin function, have remained unresolved. Here, we show that optovin's photophysics in solution are governed by competition between rapid photoisomerization and intersystem crossing. Violet-light excitation prepares the bright $S_2(\pi\pi^*)$ state, which rapidly relaxes over picoseconds to the dark $S_1(n\pi^*)$ state. Most excited molecules subsequently decay through torsional *Z*-*E* photoisomerization over tens of picoseconds, providing a reversible nonradiative pathway. In parallel, a minor fraction (10−30% depending on solvent) of the excited-state population undergoes intersystem crossing to form a short-lived triplet state that persists for up to a nanosecond. Direct near-infrared detection of singlet oxygen confirms triplet-mediated oxygen sensitization, although with a low apparent quantum yield of a fraction of a percent, with no dependence on the initial isomeric composition of optovin. These results identify competition between torsional internal conversion and intersystem crossing as the central branching process in optovin photophysics. These intrinsic excited-state dynamics provide experimentally defined constraints on models of TRPA1 activation and establish photophysical design principles for next-generation, gene-free optopharmacological agents.



INTRODUCTION

Optogenetics utilizes light as a control element for manipulating neuronal activity with high spatiotemporal precision.[1−4] Building on this foundation, optopharmacology aims to extend optical control to native molecular targets using photosensitive small molecules, offering the prospect of reversible, cell-type-specific activity modulation without genetic modification.[5−7] Optovin (Figure 1), a founding molecule in optopharmacology, demonstrated that chemically based approaches targeting native proteins can be used for optical control.[6,8−10]

The first demonstration of optovin's function in juvenile zebrafish larvae showed selectivity toward the TRPA1 ion channel responsible for mediating transduction of pain signals in sensory neurons[11,12] where, upon violet-light stimulation, control over channel activation and neuronal depolarization could be achieved. The utility of optovin has been demonstrated beyond zebrafish, including *in vivo* photostimulation in mice, and extension to cardiac control where brief violet-light pulses were used to rhythmically pace photoexcitable tissue containing TRPA1, providing an optopharmacological route to optical pacing without microbial opsins.[13−15] In addition to *in vivo* pacing, the same TRPA1-optovin strategy can drive optical pacing in human (stem cell) cardiomyocytes *in vitro*, potentially allowing for optical control of human electrophysiology.[14] Localized two-photon activation

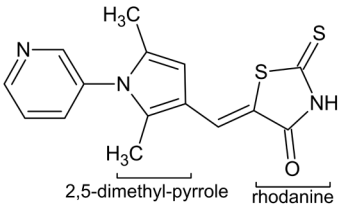


Figure 1. Molecular structure of optovin, highlighting the rhodanine and substituted 2,5-dimethyl-pyrrole units. In juvenile zebrafish, optovin acts through the TRPA1 (transient receptor potential ankyrin 1) ion channel,[13,19] which mediates the transduction of pain signals in sensory neurons.[11,12] The mechanism of ion channel activity photomodulation is thought to involve light-dependent covalent modification of cysteine residue(s) in the ion channel following absorption of violet light.[13,14] The lowest energy geometric isomer has *Z* configuration about the methylene bridge bond. Note that the pyridine ring is perpendicular to the plane defined by the rhodanine-dimethylpyrrole groups due to steric interactions.

Received: June 30, 2026
Revised: October 9, 2026
Accepted: October 13, 2026

ACS Publications
© XXXX The Authors. Published by American Chemical Society

Downloaded from pubs.acs.org/jacsat/article-pdf/doi/10.1021/jacs.6c13271/6905279/jacs.6c13271.pdf by UNIV OF EAST ANGLIA user on 03 November 2026

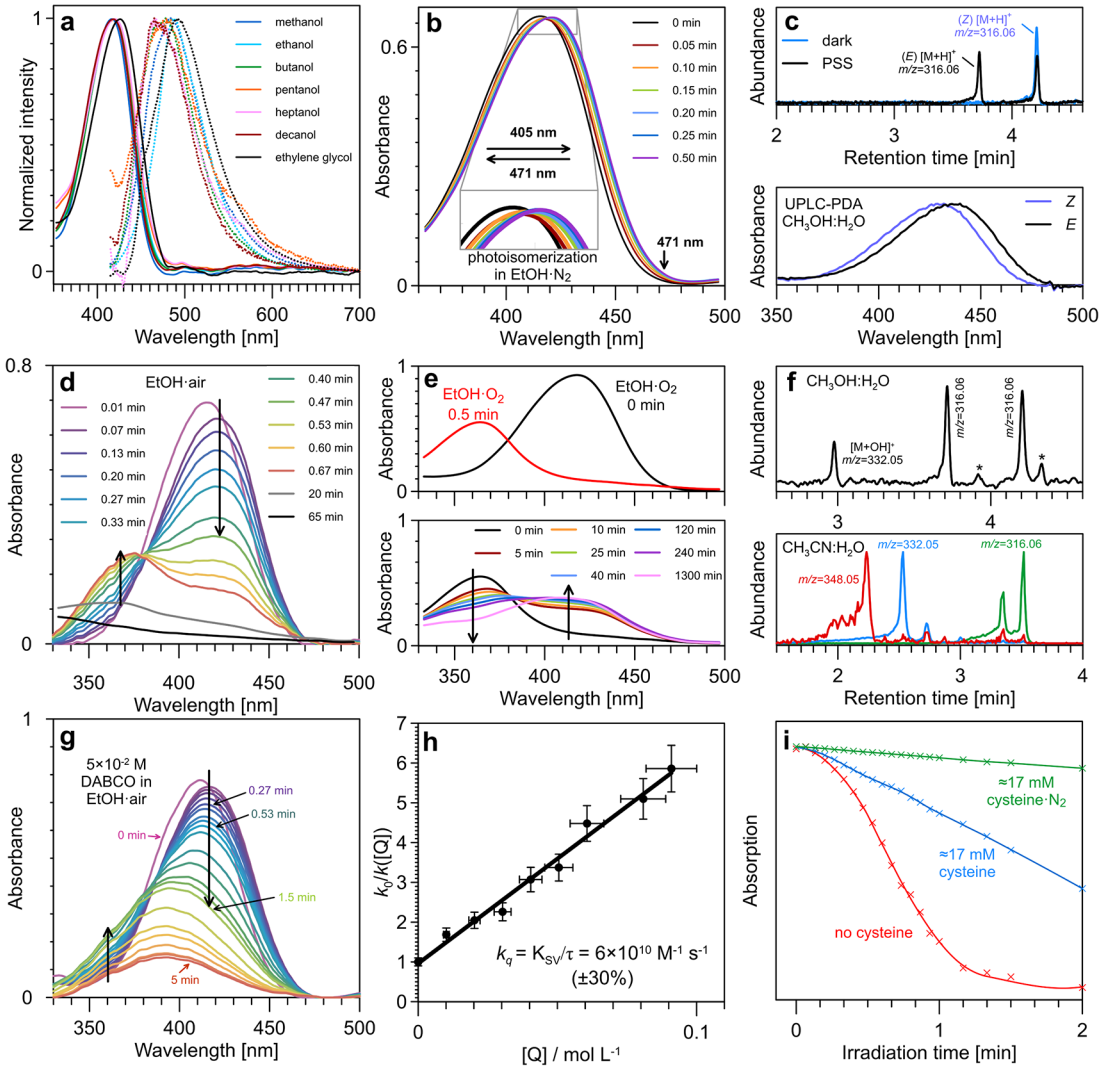


Figure 2. Photoswitching and triplet-mediated photoreactions of optovin: (a) Absorption and fluorescence emission spectra in protic solvents. Emission spectra were recorded out to 1000 nm (700−1000 nm region not shown), with no evidence for phosphorescence. See Figure S4 for aprotic solvents. (b) Irradiation (405 nm LED) of optovin in ethanol purged with nitrogen, demonstrating *Z*-*E* photoisomerization to reach a photostationary state (PSS). Irradiation of the 1.0 min PSS solution with 471 nm laser light for 20 s, regenerated the initial absorption spectrum. (c) UPLC-MS of the initial N_2-purged solution and a PSS solution, identifying the *Z* and *E* isomers (upper). UPLC-PDA spectra of the eluting components (lower). (d) Irradiation of optovin in aerated ethanol, demonstrating rapid loss of the optovin absorption band at ≈400 nm and formation (with longer-time scale loss) of a photoproduct band at ≈365 nm. (e) Irradiation of optovin in oxygen-saturated ethanol showed rapid photoreaction (upper), with partial thermal recovery (lower) consistent with an irreversible photochemical fatigue pathway. (f) UPLC-PDA chromatogram with a CH_3OH:H_2O mobile phase showing singly oxygenated (*m*/*z* 332.05) optovin (upper), with doubly oxygenated optovin (*m*/*z* 348.05, lower) probably at a range of oxygenation sites based on the breadth of the UPLC peak. The *m*/*z* 348.05 species is sparingly soluble in CH_3OH and elutes at the solvent front. (g) Selected absorption spectra of optovin in aerated ethanol with DABCO triplet quencher and 405 nm irradiation, showing delayed photoreaction. (h) Stern−Volmer analysis of optovin in aerated ethanol with DABCO. (i) Photoreaction quenching effect of optovin with cysteine in methanol.

of optovin in rat cortical neurons has further shown that optovin-mediated TRPA1 activation can be spatially confined to neuronal subcompartments using near-infrared excitation.[16] More recently, visible-light photoswitchable aryl azopyrrole TRPA1 ligands have expanded this chemogenetic strategy, providing red-shifted TRPA1 control in live zebrafish larvae.[17]

Despite optovin's pivotal role as a small-molecule tool for gene-free optical control of native ion channels,[18] the primary excited-state pathway that enables TRPA1 activation remains unresolved. Point-mutation studies implicating Cys621, Cys633, and Cys856 in TRPA1 activity indicate that optovin function depends on cysteine residues, consistent with the broader role of electrophile-sensitive cysteines in TRPA1 activation,[13,19] while singlet-oxygen ($^1O_2$) sensitization suggested the generation of reactive oxygen species (ROS) as $^1O_2$ but not hydroxyl radicals or superoxide. Taken together, these observations raised two mechanistic possibilities: direct photoreaction following optovin binding to TRPA1, or an indirect $^1O_2$-mediated pathway. However, behavioral assays in zebrafish cotreated with DABCO, a $^1O_2$ quencher and efficient triplet energy acceptor,[20] showed complete suppression of the optovin photoresponse, while TRPA1 measurements using other $^1O_2$-generating compounds exhibited no photoactivity. Because DABCO can quench both $^1O_2$ and excited triplet states, these observations do not by themselves identify the reactive intermediate, but they indicate that optovin activity is

https://doi.org/10.1021/jacs.6c13271
J. Am. Chem. Soc. XXXX, XXX, XXX−XXX

Downloaded from pubs.acs.org/jacsat/article-pdf/doi/10.1021/jacs.6c13271/6905272 9/jacs.6c13271.pdf by UNIV OF EAST ANGLIA user on 03 November 2026

Table 1. Spectral Properties and Excited-State Lifetimes of *Z*-Optovin[a]

solvent	λ_{abs}	λ_{em}	$\Delta\tilde{\nu}$	ε	η	$\tau_{F,1}$	$\tau_{F,2}$	τ_1	τ_2	τ_3
methanol	420	483	3105	33.0	0.54	0.6 ± 0.1	5.5 ± 0.3	0.5 ± 0.1	6.3 ± 0.4	423 ± 69
ethanol	420	486	3233	25.3	1.07	0.6 ± 0.1	5.6 ± 0.3	—	—	—
butanol	419	478	2945	17.8	2.54	0.7 ± 0.1	5.4 ± 0.3	—	—	—
pentanol	421	479	2876	15.1	3.62	0.6 ± 0.1	5.5 ± 0.3	—	—	—
heptanol	421	465	2248	11.8	5.81	0.7 ± 0.1	5.7 ± 0.3	—	—	—
decanol	421	465	2247	7.9	10.91	0.7 ± 0.1	5.8 ± 0.3	—	—	—
ethylene glycol	430	492	2930	41.1	16.06	1.2 ± 0.1	14 ± 1	1.3 ± 0.2	31 ± 5	1200 ± 200
acetonitrile	421	492	3427	36.6	0.37	1.3 ± 0.1	10.2 ± 0.8	0.4 ± 0.1	12.4 ± 0.8	505 ± 64
ethyl acetate	419	465	2360	6.1	0.42	0.8 ± 0.1	4.9 ± 0.3	—	—	—
tetrahydrofuran	421	466	2293	7.5	0.46	0.9 ± 0.1	5.3 ± 0.4	0.6 ± 0.1	5.9 ± 0.5	401 ± 65
dimethyl sulfoxide	402	449	2603	47.2	1.99	1.2 ± 0.2	15 ± 2	0.9 ± 0.2	13.1 ± 0.9	581 ± 51

[a]Absorption (abs) and fluorescence emission (em) maxima, in nm (±2 nm), recorded at room temperature (T = 294 K). The fluorescence excitation wavelength was 400 nm. Stokes shift ($\tilde{\Delta}\nu$ for band maxima) is given in cm^{-1} (±10 cm^{-1}). ε is the solvent dielectric constant, and η is viscosity in cP. Lifetimes $\tau_{F,1}$ and $\tau_{F,2}$ are from fits of femtosecond fluorescence upconversion measurements, while τ_1, τ_2, and τ_3 were derived from fits of transient absorption spectroscopy.

unlikely to arise from nonspecific condensed-phase $^1O_2$ generation alone. One possible interpretation is a model in which optovin preassociates with TRPA1 and undergoes a photoreaction at, or near, cysteine residues, with Cys621, Cys633, and Cys856 implicated by previous mutagenesis studies.

A key unresolved question is how does optovin operate at the molecular level? Namely, what excited-state branching process inherent in a freely diffusing photoswitch allow it to become a site-directed TRPA1 photochemical tool? Establishing the branching mechanism between reactive and nonreactive channels is necessary both for understanding optovin's biological activity and for guiding the design of improved optopharmacological photoswitches. The thione group as part of the rhodanine unit in optovin is chemically notable because thione-containing chromophores often exhibit enhanced spin–orbit coupling and efficient access to triplet states.[21−24]

Here, we characterize the photochemistry and ultrafast excited-state dynamics underlying optovin's photomechanism, revealing a bifurcation of the excited-state population: following picosecond relaxation away from the Franck–Condon state, the dominant fraction returns to the ground electronic state through a twisted-geometry conical-intersection seam, while a smaller fraction undergoes intersystem crossing to a short-lived yet reactive triplet state. We propose that the optopharmacological activity may favor preassociation of optovin within a binding environment, consistent with rapid deactivation when the chromophore is not preoriented near a suitable cysteine residue. Therefore, optovin's optopharmacological specificity is proposed to be due to the interplay between molecular recognition and excited-state dynamics that give rise to the photoreactive channel. This mechanistic framework identifies the triplet state as a key designable intermediate rather than an incidental photophysical product,[25−27] providing direction for developing derivative optopharmacological agents.

RESULTS AND DISCUSSION

Photoswitching and Triplet-Induced Photoreactivity

Optovin absorbs UV-blue light across the 350–450 nm range in common organic solvents (Figures 2a and S4, Tables 1 and S2), with a high molar absorptivity (≈65,000 L mol^{-1} cm^{-1}, Figure S6). Fluorescence is weak with measured quantum yield at $\Phi_F \approx 10^{-4}$ in ethanol, indicating efficient nonradiative decay of the initial excited state. The wavelength of maximum absorption is insensitive to solvent polarity or hydrogen-bonding capacity (Table S3), and the Stokes shift broadly increases with increasing solvent polarity. In nitrogen-purged solvents where dissolved oxygen is minimized, optovin showed *Z*-*E* photoswitching following absorption of blue light (405 nm), evidenced by a slightly red-shifted absorption spectrum (Figure 2b). This transformation was confirmed with UPLC-MS and photodiode array (PDA) analysis (Figure 2c), where the photostationary state (PSS) contains two isomers with strongly overlapping absorption spectra as recorded by UPLC-PDA. ^{1}H NMR spectra (Figure S11) are consistent with a single starting isomer and a 45:55% isomer PSS ratio. Photoswitching of optovin was reversible in all solvents using monochromatic laser light at 471 nm, exciting on the red edge of the PSS spectrum, and observing recovery of the initial absorption spectrum. In solvents purged with nitrogen gas, reversible photoswitching was achieved more than 10 times with no or minimal degradation (Figure S5).

In aerated (Figure 2d) or oxygenated (Figure 2e, upper) solvents, optovin not only photoswitches but also photoreacts leading to loss of its absorption band and growth of a photoproduct band centered at ≈365 nm. The photoreaction rate was drastically enhanced in oxygenated solvents, and was only partially thermally reversible (Figure 2e, lower). UPLC-MS (Figure 2f) confirmed that the photoreaction generated adducts consistent with single (m/z 332.05) and double (m/z 348.05) oxygen addition, with the latter showing poor solubility in methanol compared with acetonitrile and some extent of thermal reversion. One plausible assignment for the doubly oxygenated m/z 348.05 species is 2,5-addition across the pyrrolic moiety to form an endoperoxide-like product,[28,29] although the precise oxygenation site(s) could not be assigned from UPLC-MS alone.

The photoreaction coordinate in aerated solvents could be slowed with addition of triplet-quencher DABCO (Figure 2g). No DABCO effect was observed in nitrogen-purged solutions, consistent with a triplet photoreaction process in oxygenated solvents. Stern–Volmer-type analysis of the DABCO quenching effect of the photoreaction in aerated ethanol ($[O_2] \approx 1.9$ mM at T = 298 K)[30] gave a near monotonic dependence on quencher concentration,[31,32] consistent with triplet-state quenching dynamics. Using the triplet lifetime from our ultrafast spectroscopy (≈500 ps, see below), the slope

https://doi.org/10.1021/jacs.6c13271
J. Am. Chem. Soc. XXXX, XXX, XXX−XXX

Downloaded from pubs.acs.org/jacsat/article-pdf/doi/10.1021/jacs.6c13271/69052729/jacs.6c13271.pdf by UNIV OF EAST ANGLIA user on 03 November 2026

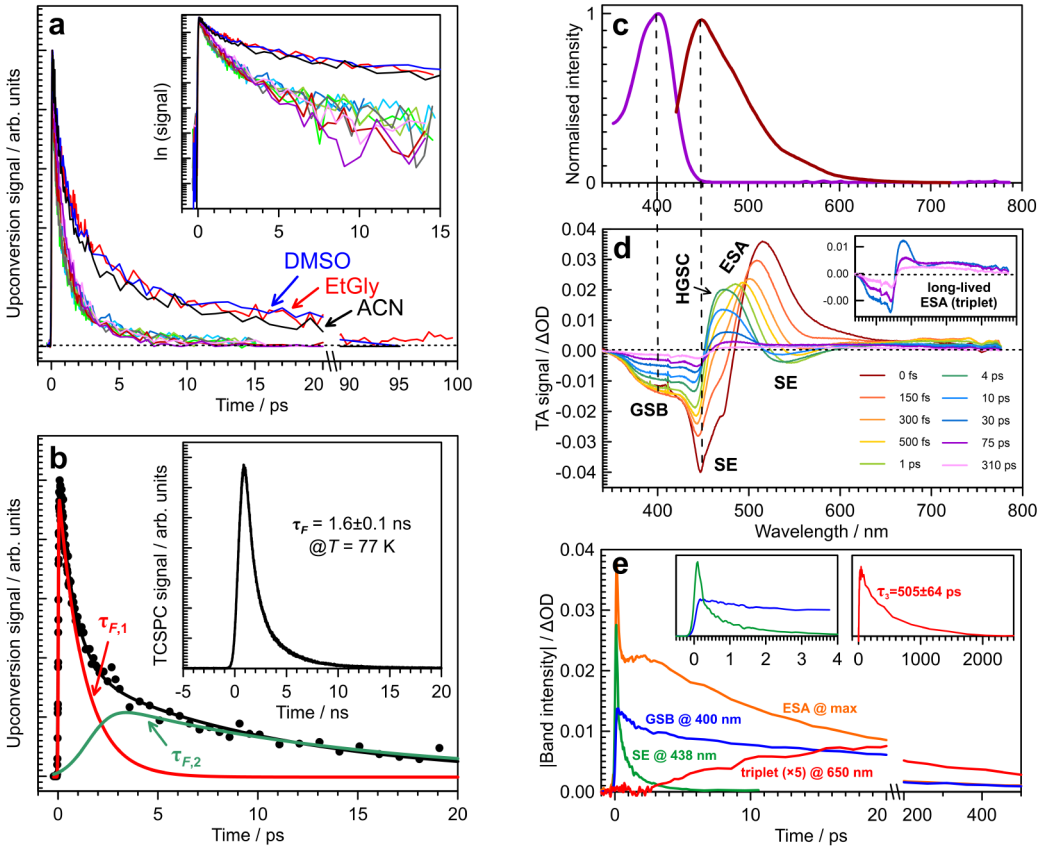


Figure 3. Excited-state dynamics of optovin: (a) Ultrafast fluorescence upconversion decays measured in each solvent listed in Table 1. The inset shows a logarithmic vertical abscissa scale, which clearly reveals nonmonoexponential decay and no viscosity effect. ACN—acetonitrile, EtGly—ethylene glycol, and DMSO—dimethyl sulfoxide form a grouping with similar decay lifetimes. (b) Fit of the acetonitrile upconversion data with a two-component exponential decay, returning $\tau_{F,1}$ and $\tau_{F,2}$ (inset at $T \approx 77$ K). (c) Absorption (purple) and fluorescence emission (maroon, 400 nm pump) spectra in acetonitrile. (d) Selected TA spectra in acetonitrile (420 nm excitation): GSB—ground-state bleach, SE—stimulated emission, ESA—excited-state absorption, HGSC—hot ground-state cooling. The inset shows weak, long-lived ESA extending to ≈780 nm with trace amounts remaining for >1 ns. (e) Representative TA kinetics in acetonitrile at selected wavelengths from which a sequential model $\mathbf{1} \xrightarrow{\tau_1} \mathbf{2} \xrightarrow{\tau_2} \mathbf{2} \xrightarrow{\tau_3} S_0$ provided the lifetimes in Table 1.

corresponds to an apparent quenching rate constant of $k_q \approx 6 \times 10^{10}$ M^{-1} s^{-1}, close to the diffusion-controlled limit in ethanol.[33] The oxygen-dependent photoreaction quantum yield was $\approx 10^{-3}$. However, this value should be regarded as a product-formation yield rather than a direct measure of the intersystem crossing (ISC) yield, because the short intrinsic triplet lifetime (see below) means that only a small fraction of triplets are intercepted by dissolved oxygen before decay. For a diffusion-controlled reaction with oxygen, we estimate an ISC quantum yield of <20%, consistent with values for thione-containing organic dyes exhibiting fast triplet-formation ISC lifetimes (ca. 10 ps).[25,26,34] Similar photoreaction and quenching kinetics were observed for optovin in acetonitrile (Figure S8).

Further evidence for population of the triplet manifold was obtained through direct detection of the characteristic near-infrared emission from singlet oxygen ($^1O_2$, Figure S10). Upon 405 nm excitation of optovin in aerated acetonitrile, $^1O_2$ emission was observed, confirming that optovin can sensitize molecular oxygen through its triplet state. The apparent singlet-oxygen sensitization quantum yield was low, $\Phi_\Delta \approx 0.1$–0.2%, consistent with a short intrinsic triplet lifetime limiting interception by dissolved O_2. Measurements starting from a *Z*-isomer sample and from the 415 nm PSS gave comparable absorption-corrected $^1O_2$ emission intensities, indicating no significant dependence of sensitization efficiency on the initial isomeric composition. This suggests that both *Z*- and *E*-isomers retain access to the triplet manifold under photoirradiation, which is expected since their individual absorption spectra differ by only ≈10 nm (Figure 2c, lower).

Previous biological studies have implicated Cys621, Cys633, and Cys856 in TRPA1 activation by optovin,[13] although the molecular role of these residues remains unresolved. Importantly, cysteine is not required to promote ISC in optovin, rather, triplet formation is an intrinsic property of optovin. Addition of free cysteine to aerated methanol efficiently suppressed optovin photodegradation (Figure 2i), but UPLC-MS revealed no distinct stable optovin-cysteine photoproduct. Thus, the present solution measurements do not establish whether cysteine acts as a direct photochemical reaction partner, contributes to molecular recognition and positioning of optovin, or influences the photochemistry through another mechanism. Nevertheless, they show that cysteine can modulate the photochemistry of the intrinsically generated optovin triplet state, providing a plausible link between the condensed-phase excited-state dynamics identified here and the cysteine dependence observed in TRPA1 activation.

https://doi.org/10.1021/jacs.6c13271
J. Am. Chem. Soc. XXXX, XXX, XXX−XXX

Downloaded from pubs.acs.org/jacsat/article-pdf/doi/10.1021/jacs.6c13271/69052729/jacs.6c13271.pdf by UNIV OF EAST ANGLIA user on 03 November 2026

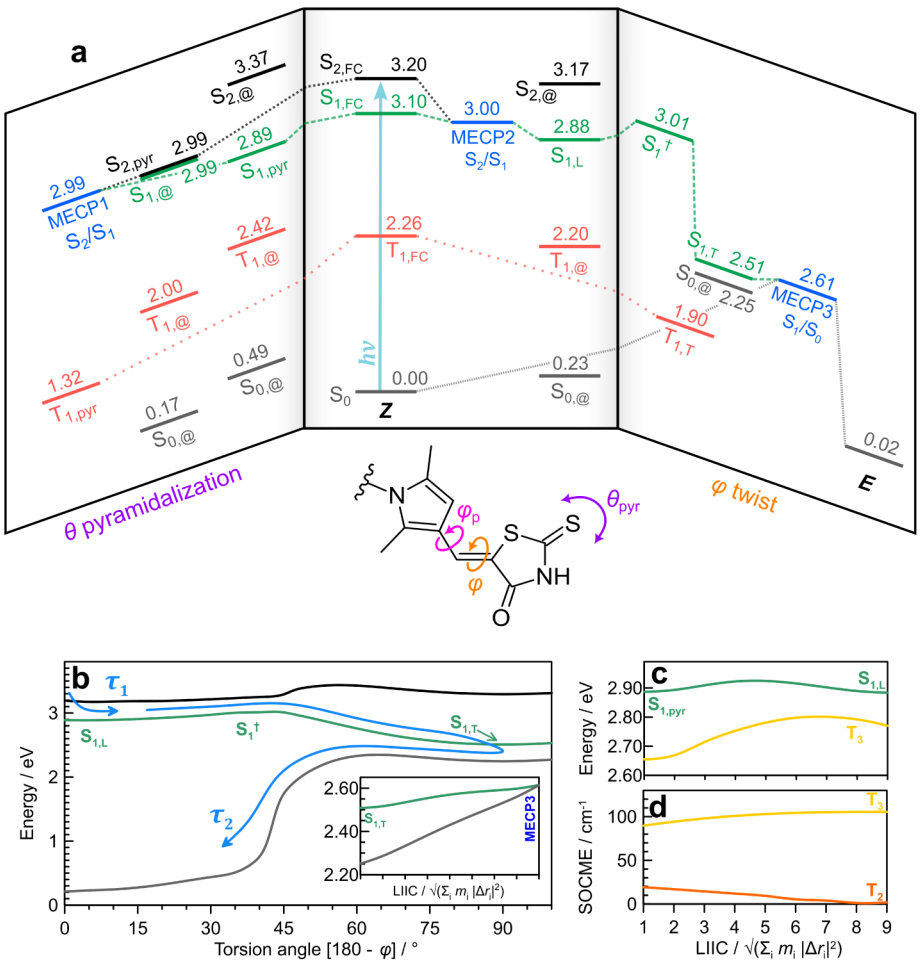


Figure 4. Potential energy surface for the excited state dynamics of *Z*-optovin (black—S_2, green—S_1, red—triplet, blue—conical intersection): (a) Critical points in the context of the two most significant geometric parameters, φ as torsion about the double bond and θ_{pyr} as pyramidalization of the carbon atom on the thione functionality (structures in Figure S20). (b) Relaxed potential energy surface along the φ coordinate (φ = 180° for the *Z*-isomer). A photon excites to the planar Franck−Condon (FC) $S_2(\pi\pi^*)$ state. Small scale, barrierless motion connects $S_{2,FC}$ with two MECPs, MECP1 along the θ_{pyr} coordinate and MECP2 retaining a near planar geometry. These MECPs lead to the nonfluorescent $S_{1,pyr}$ and $S_{1,L}$ states, respectively, with this decay assigned to lifetime τ_1. A twisted $S_{1,T}$ state is in close geometric and energetic proximity to an isomerizing conical intersection (MECP3 in b, inset), and is linked with lifetime τ_2. (c) Mass-weighted linear interpolation in internal coordinates (LIIC) of the S_1 state potential energy surface between $S_{1,pyr}$ and $S_{1,L}$ state geometries and nearby T_3 triplet state, revealing a near-barrierless pathway. (d) Spin−orbit coupling matrix element (SOCME) norms along the LIIC suggest moderate T_3-S_1 coupling facilitating intersystem crossing. The τ_2 lifetime is therefore assigned to competitive loss of S_1 population by torsional motion through MECP3 and by ISC near the $S_{1,pyr}/S_{1,L}$ state region.

Ultrafast Excited-State Dynamics and ISC Gateway

The excited-state dynamics responsible for optovin's photoswitching and triplet state formation were uncovered using ultrafast fluorescence upconversion and transient absorption (TA) spectroscopies (Figure 3), interpreted against calculated excited-state potential energy surfaces (Figure 4) that reveal a bright $S_2(\pi\pi^*)$ state lying close in energy to a dark $S_1(n\pi^*)$ state, an extended S_1/S_0 conical-intersection region along the isomerization coordinate, and a nearby ISC-active region providing access to the triplet manifold.

Ultrafast fluorescence upconversion (Figure 3a), which is suited to monitoring the fastest of the initial dynamics, shows that the fluorescing state decays over a few picoseconds, consistent with the low fluorescence quantum yield at $\Phi_F \approx 10^{-4}$. There is no obvious dependence of fluorescence upconversion data on bulk solvent parameters, including viscosity, polarity, or hydrogen-bonding capacity. Rather, fluorescence lifetimes fall into two groups: (i) ethyl acetate, tetrahydrofuran, and all alcohols except ethylene glycol, and (ii) acetonitrile, dimethyl sulfoxide, and ethylene glycol. All fluorescence decay profiles are biexponential (logarithmic axis inset in Figure 3a), and were readily fit with a sequential two component exponential decay, $\mathbf{1} \xrightarrow{\tau_{F,1}} \mathbf{2} \xrightarrow{\tau_{F,2}} \mathbf{dark}$ (Figure 3b), providing $\tau_{F,1}$ and $\tau_{F,2}$ lifetimes (Table 1). We interpret the $\tau_{F,1}$ lifetime at ≈1 ps as impulsive loss of the fluorescent Franck−Condon state, and the $\tau_{F,2}$ lifetime as loss of S_2 population farther from the conical-intersection seam (e.g., S_2−S_1 potential energy surfaces are approximately parallel along the first ≈ 45° of the φ coordinate, Figure 4b). From the potential energy surface (Figure 4), loss of the fluorescent state is linked with internal conversion from the initially excited $S_2(\pi\pi^*)$ state to either the lower-lying, dark $S_1(n\pi^*)$ state along the θ_{pyr} pyramidization coordinate (left-hand pathway in Figure 4a) leading to the $S_{1,pyr}$ geometry or along the φ coordinate (right-hand pathway in Figure 4a) leading to the $S_{1,L}$ geometry. Because of the near degeneracy of S_2 and S_1 states at the Franck−Condon geometry, and because either internal conversion pathway requires very little nuclear motion from

https://doi.org/10.1021/jacs.6c13271
J. Am. Chem. Soc. XXXX, XXX, XXX−XXX

Downloaded from pubs.acs.org/jacsat/article-pdf/doi/10.1021/jacs.6c13271/6905272 9/jacs.6c13271.pdf by UNIV OF EAST ANGLIA user on 03 November 2026

the Franck−Condon state, little to no dependence of decay lifetime on bulk solvent parameters (viscosity, polarity) is expected. The two groupings of fluorescence lifetimes must be due to specific solute−solvent interactions, for example, stabilizing the $S_1(n\pi^*)$ state for the second grouping.[35] Nonadiabatic molecular dynamics trajectories confirmed a S_2-S_1 internal conversion with lifetime τ_{decay} = 1.1 ± 0.1 ps (Figure S20), consistent with experiment, finding internal conversion occurs along a seam near degenerate with the pathway connecting the $S_{1,pyr}$ and $S_{1,L}$ state geometries, but are slightly weighted toward forming the $S_{1,L}$ geometry.

TA spectroscopy was used to follow the dynamics over the entire excited-state profile. Selected TA spectra in acetonitrile (Figure 3d, see Figures S16 and S17 for other solvents) show bands assigned to ground state bleach (GSB), stimulated emission (SE), excited-state absorption (ESA) that overlaps with the SE band, HGSC, and a broadband, long-lived ESA band. The GSB and ESA bands are fully consistent with calculated excited-state absorption spectra assuming explicitly solvated molecular structures, allowing for definitive band assignments (Figure S19). Over the first few hundred femtoseconds, the pronounced ESA band at ≈515 nm blue shifts and reshapes, reaching a wavelength maximum at ≈470 nm after several picoseconds. This evolution is consistent with $S_2(\pi\pi^*)$ to $S_{1,L}$ state internal conversion, but the later-time band shape is also expected to contain a contribution from hot ground-state cooling (HGSC) following rapid nonradiative decay.[36,37] The red edge of the SE band becomes evident during this reshaping, with the SE band lost after ≈10 ps, consistent with the $\tau_{F,2}$ lifetimes from ultrafast fluorescence upconversion measurements (Table 1).

Over longer time scales, trace amounts of GSB and ESA are evident extending out to several nanoseconds (≈1% transient signal level at 1.1 ns), consistent with the small extent of ISC and triplet-state formation independently identified from DABCO quenching and direct $^1O_2$ sensitization measurements. Taking band integrations and applying Franck−Condon ($S_{2,FC}$), $S_{1,L}$, and $T_{1,T}$ state geometry absorption cross sections calculated at 5.3×10^{-16}, 2.7×10^{-16}, and 3.0×10^{-16} cm^2, respectively, the ratiometric triplet yields are ≈9% in acetonitrile (consistent with extent of remaining GSB after some tens of picoseconds), ≈20% methanol, THF, and DMSO, and <30% in ethylene glycol. The estimated uncertainty in these triplet yields is conservatively taken as approximately ±20% relative, reflecting uncertainties in the calculated absorption cross sections and band integrations, for example, the triplet yield in acetonitrile is 9 ± 2%. TA measurements of flowing optovin in methanol or acetonitrile containing DABCO (10 mM), or in oxygen-saturated methanol, returned near-identical spectra and lifetimes. Thus, although DABCO measurably suppresses the accumulated oxygen-dependent photoproduct yield, bimolecular quenching does not significantly perturb the intrinsic subnanosecond excited-state kinetics under the TA conditions.

The predominant relaxation pathway of optovin once population reaches the S_1 state is through torsion about the methylene bridge coordinate φ, such that lifetime τ_2 at several to tens of picoseconds corresponds to isomerization by passage through a twisted-geometry conical-intersection seam (Figure 4b).[38] The longer τ_2 lifetime in ethylene glycol (≈31 ps) confirms that this coordinate shows a weak viscosity dependence as expected for a volume-conserving isomerization processes in a monomethine system.[39,40] Triplet formation must therefore compete directly with torsional internal conversion. The near-degenerate $S_{1,L}$ and $S_{1,pyr}$ state geometries, separated by only a small barrier of ≈4 meV (Figure 4c), lie close in energy to the $T_3(\pi\pi^*)$ state and have substantial spin−orbit coupling matrix element norms of 90−100 cm^{-1} (Figure 4d)—these values are large for an organic chromophore, but are consistent with sulfur-substituted heterocycles, where values are ≈100 cm^{-1} for 2-thiothymine, ≈150 cm^{-1} for 4-thiothymine, and 157−160 cm^{-1} for thiouracil/thiouridine derivatives.[41−43] This region of the S_1 state surface thus provides an efficient ISC gateway, allowing a minor fraction of the excited-state population to reach the triplet manifold before it can overcome the low $S_1^\dagger$ isomerization barrier (≈13 meV). The observed triplet yield is therefore determined by bifurcation between rapid torsional internal conversion and ISC from the S_1 state potential energy surface.

Implications for Optovin Function in TRPA1

The condensed-phase measurements identify a general mechanism by which a local molecular environment could modulate the excited-state branching of optovin. Torsional motion about the methylene bridge provides the dominant S_1 state decay pathway, and restricting this coordinate slows internal conversion and allows ISC to compete more effectively. This behavior is evident in ethylene glycol, where the longer S_1 state lifetime is accompanied by an increased triplet yield. Whether binding to TRPA1 produces such a restriction is presently unknown because the optovin binding site and bound geometry have not been established. Recent time-resolved studies of protein-bound photoswitches have shown that ligand motion and photochemical outcome can be strongly shaped by the local protein environment.[44] A useful analogy is provided by the green fluorescent protein (GFP) chromophore. The GFP chromophore is only weakly fluorescent because rapid torsional motion drives nonradiative photoisomerization in both solution and the gas phase,[45,46] whereas encapsulation within the protein's β-barrel restricts isomerization and leads to excited-state proton transfer and bright fluorescence.[47,48] By analogy, conformational restriction of optovin in a TRPA1 binding environment provides a plausible means of modulating the competition between torsional internal conversion and ISC.

The short lifetime of the optovin triplet state places an important kinetic constraint on any mechanism involving this reactive channel. With a lifetime of several hundred picoseconds in solution, an optovin triplet state generated freely in solution is unlikely to encounter a specific protein reaction site by diffusion before intrinsic decay or quenching. Thus, if the triplet state contributes to TRPA1 activation, preassociation of optovin with the protein would provide a plausible means of positioning the chromophore close to residues that influence its ensuing photochemistry. This interpretation is consistent with the previously reported sensitivity of optovin activity to mutation of specific cysteine residues and suppression by DABCO, while other singlet-oxygen-generating compounds do not reproduce optovin activity.[13,14,20] Together with the low singlet-oxygen sensitization yield measured here, these observations favor a role for molecular recognition in optovin function over nonspecific condensed-phase ROS generation, although the molecular role of the implicated cysteine residues remains unresolved. A proximity-gated mechanism of this type has precedent in chemical biology, where short-lived reactive

Downloaded from pubs.acs.org/jacsat/article-pdf/doi/10.1021/jacs.6c13271/69052729/jacs.6c13271.pdf by UNIV OF EAST ANGLIA user on 03 November 2026

https://doi.org/10.1021/jacs.6c13271
J. Am. Chem. Soc. XXXX, XXX, XXX−XXX

intermediates are widely exploited to achieve target-selective photochemistry from preassociated complexes.[49−54] Although the reactive intermediate in optovin is different, the kinetic selectivity principle is analogous. In this sense, the short triplet lifetime may contribute to optovin specificity.

The activity screening of optovin analogues in juvenile zebrafish indicated that both the pyrrole and rhodanine-thione units are important for optovin activity.[13] Removal of the pyrrole ring, or replacement with a dimethylaniline group, inhibited optopharmacological activity, indicating that the electronic and geometric properties of this part of the conjugated chromophore are important for function. Similarly, modifications to the rhodanine ring, which contains the thione unit implicated here in triplet-state formation also caused loss of activity. Notably, replacement of the thione with a carbonyl, which is expected to alter both the singlet−triplet energetic landscape and the spin−orbit coupling associated with the sulfur-containing chromophore,[22] inhibited activity. However, interestingly, retention of activity for a hydantoin-containing analogue shows that the precise rhodanine-thione structure is not an absolute requirement for photoactivity, but rather that this region of the molecule is highly sensitive to changes that alter the excited-state landscape. In contrast, replacement of the pyridine ring with a methyl group retained activity, consistent with the pyridine substituent being less central to the intrinsic excited-state branching coordinate. These structure−activity trends suggest that the pyrrole and rhodanine-thione units are central to the combination of TRPA1 recognition, excited-state branching, and optopharmacological activity. The pyridine unit in optovin may therefore represent a synthetically useful direction for red-shifting absorption and tuning the excited-state potential energy surface, provided that modifications preserve the molecular recognition and excited-state properties important for optovin function. Understanding this connection establishes a route toward improved optopharmacological agents in which binding affinity, local excited-state dynamics, and triplet reactivity are co-optimized.

CONCLUSIONS

The photochemistry of optovin in solution has revealed the intrinsic excited-state pathways that will influence its optopharmacological behavior in TRPA1. Following blue-light excitation to the bright $S_2(\pi\pi^*)$ state, optovin undergoes ultrafast internal conversion to the dark $S_1(n\pi^*)$ state. When in solution, most of the excited-state population then returns to the ground state through torsional motion about the methylene bridge, allowing for reversible *Z-E* photoswitching. In parallel, a minor fraction undergoes ISC to form a short-lived triplet state. Although this triplet channel is inefficient in free solution, it accounts for the oxygen-dependent photoreactivity and DABCO quenching, with direct detection of singlet-oxygen emission providing further evidence that it forms a chemically reactive channel in optovin's excited-state manifold.

The central mechanistic implication is that optovin activity in TRPA1 may be linked with the combination of molecular recognition and environment-controlled excited-state dynamics. Because the triplet state survives for a nanosecond or less in solution, any mechanism involving this reactive channel would favor preassociation with TRPA1 in a geometry that positions the chromophore near residues capable of influencing its ensuing photochemistry. Binding may therefore both position optovin for local photochemistry and restrict the torsional photoisomerization coordinate sufficiently to increase competition from ISC and triplet formation. Future work should investigate optovin in TRPA1 to explore the precise optovin-protein coordination and role of the cysteine residues implicated by previous biological studies.

This understanding provides several design principles for next-generation optovin derivatives and related gene-free optopharmacological tools. First, structural and computational studies of the optovin-TRPA1 binding site will be needed to identify the noncovalent interactions that preorganize the chromophore and establish the role of the implicated cysteine residues. Second, chemical modification should aim to tune the excited-state potential energy surface by raising the barrier for torsional internal conversion, stabilizing the ISC-accessible region, or increasing intrinsic spin−orbit coupling, thereby increasing the yield of the triplet channel relative to competing internal conversion. Third, absorption should be red-shifted toward the bio-optical window[55−60] to improve tissue compatibility, while preserving the molecular recognition and excited-state properties important for optovin function. Finally, the short triplet lifetime should not necessarily be viewed as a limitation, rather it may be an important feature that suppresses nonspecific ROS generation while retaining access to a chemically reactive triplet channel.

ASSOCIATED CONTENT

Supporting Information

The Supporting Information is available free of charge at https://pubs.acs.org/doi/10.1021/jacs.6c13271.

Materials, experimental and theoretical methods, summary of isomers and rotamers, spectrophotometry in all solvents, low-temperature fluorescence spectroscopy, singlet-oxygen emission and quantum-yield measurements, ^{1}H NMR spectra, fluorescence upconversion power dependence, summary of excited-state lifetimes with bulk solvent parameters, transient absorption spectra in methanol, ethylene glycol, THF, and DMSO, TA spectral fit examples, TA spectral band simulations with explicit potential energy surface solvation, and NAMD trajectories for $S_2 \rightarrow S_1$ internal conversion (PDF)

AUTHOR INFORMATION

Corresponding Author

James N. Bull − *Chemistry, Faculty of Science, University of East Anglia, Norwich NR4 7TJ, United Kingdom;* orcid.org/0000-0003-0953-1716; Email: james.bull@uea.ac.uk

Authors

Jonathan Q. Brouwer − *Stratingh Institute for Chemistry, University of Groningen, Groningen 9747 AG, The Netherlands;* orcid.org/0009-0004-0536-7220

Alex J. Cook − *Chemistry, Faculty of Science, University of East Anglia, Norwich NR4 7TJ, United Kingdom*

Eleanor K. Ashworth − *Chemistry, Faculty of Science, University of East Anglia, Norwich NR4 7TJ, United Kingdom;* orcid.org/0000-0003-4805-4860

Anam Fatima − *Chemistry, Faculty of Science, University of East Anglia, Norwich NR4 7TJ, United Kingdom;* orcid.org/0000-0003-2388-4390

https://doi.org/10.1021/jacs.6c13271
J. Am. Chem. Soc. XXXX, XXX, XXX−XXX

Downloaded from pubs.acs.org/jacsat/article-pdf/doi/10.1021/jacs.6c13271/6905272 9/jacs.6c13271.pdf by UNIV OF EAST ANGLIA user on 03 November 2026

Khalid M. Siddiqui − *Chemistry, Faculty of Science, University of East Anglia, Norwich NR4 7TJ, United Kingdom;* orcid.org/0000-0001-6640-2406
Isabelle Chambrier − *Chemistry, Faculty of Science, University of East Anglia, Norwich NR4 7TJ, United Kingdom*
Andrew N. Cammidge − *Chemistry, Faculty of Science, University of East Anglia, Norwich NR4 7TJ, United Kingdom;* orcid.org/0000-0001-7912-4310
Pratip Chakraborty − *Chemistry, Faculty of Science, University of East Anglia, Norwich NR4 7TJ, United Kingdom;* orcid.org/0000-0002-0248-6193
Wesley R. Browne − *Stratingh Institute for Chemistry, University of Groningen, Groningen 9747 AG, The Netherlands;* orcid.org/0000-0001-5063-6961
Stephen R. Meech − *Chemistry, Faculty of Science, University of East Anglia, Norwich NR4 7TJ, United Kingdom;* orcid.org/0000-0001-5561-2782

Complete contact information is available at: https://pubs.acs.org/10.1021/jacs.6c13271

Notes

The authors declare no competing financial interest.

■ ACKNOWLEDGMENTS

This work was funded by an EPSRC New Investigator Award (EP/W018691 to JNB), an EPSRC Grant (UKRI2892 to JNB and SRM, EP/Y021525/1 and EP/X011410/1 to SRM), and the National Growth Fund Big Chemistry funded by Ministry of Education, Culture and Science (1420578 awarded to WRB). Electronic structure calculations and NAMD trajectories were carried out on the ARCHER2 UK National Supercomputing Service (https://www.archer2.ac.uk) as part of allocation e927. Mr Antony Hinchliffe, manager of the Mass Spectrometry Platform at UEA, is thanked for assistance with UPLC method development and measurements, and Dr Tony Kao is thanked for initial spectrophotometry.

■ REFERENCES

(1) Pastrana, E. Optogenetics: Controlling cell function with light. *Nat. Methods* **2011**, *8*, 24−25.
(2) Deisseroth, K. Optogenetics. *Nat. Methods* **2011**, *8*, 26−29.
(3) Emiliani, V.; Entcheva, E.; Hedrich, R.; Hegemann, P.; Konrad, K. R.; Lüscher, C.; Mahn, M.; Pan, Z.-H.; Sims, R. R.; Vierock, J.; Yizhar, O. Optogenetics for light control of biological systems. *Nat. Rev. Methods Primers* **2022**, *2* (1), 55.
(4) Miyazaki, T.; Fujino, T.; Yoshii, T.; Kosugi, H.; Funane, M.; Murata, N.; Nguyen, K. C.; Nagatoishi, S.; Tsumoto, K.; Hayashi, G.; Murakami, H.; Tsukiji, S. De novo chemo-optogenetics through the rational design of photoresponsive molecules and selection of their artificial protein binding pairs. *Nat. Chem.* **2026**, *18*, 1286.
(5) Fenno, L.; Yizhar, O.; Deisseroth, K. The development and application of optogenetics. *Annu. Rev. Neurosci.* **2011**, *34*, 389−412.
(6) Broichhagen, J.; Frank, J. A.; Trauner, D. A roadmap to success in photopharmacology. *Acc. Chem. Res.* **2015**, *48*, 1947−1960.
(7) Kobauri, P.; Dekker, F. J.; Szymanski, W.; Feringa, B. L. Rational design in photopharmacology with molecular photoswitches. *Angew. Chem., Int. Ed.* **2023**, *62* (30), No. e202300681.
(8) Qiao, Z.; Luo, J.; Tang, Y.-Q.; Zhou, Q.; Qi, H.; Yin, Z.; Tang, X.; Zhu, W.; Zhang, Y.; Wei, N.; Wang, K. Photosensitive and photoswitchable TRPA1 agonists optically control pain through channel desensitization. *J. Med. Chem.* **2021**, *64*, 16282−16292.
(9) Peng, J.; Yang, N.; Qiao, Z.; Wei, N.; Wang, K.; Zhang, Y. Photochemical control of cold−sensitive TRPA1 ion channel gating for modulation of pain sensation. *Br. J. Pharmacol.* **2025**, *182*, 3559−3576.
(10) Müller, M.; Niemeyer, K.; Ojha, N. K.; Porav, S. A.; Vinayagam, D.; Urban, N.; Büchau, F.; Oleinikov, K.; Makke, M.; Bauer, C. C.; Johnson, A. V.; Muench, S. P.; Zufall, F.; Bruns, D.; Schwarz, Y.; Raunser, S.; Leinders-Zufall, T.; Bon, R. S.; Schaefer, M.; Thorn-Seshold, O. Ideal efficacy photoswitching for chromocontrol of TRPC4/5 channel functions in live tissues. *Nat. Chem. Biol.* **2026**, *22*, 180−191.
(11) Bandell, M.; Story, G. M.; Hwang, S. W.; Viswanath, V.; Eid, S. R.; Petrus, M. J.; Earley, T. J.; Patapoutian, A. Noxious cold ion channel TRPA1 is activated by pungent compounds and bradykinin. *Neuron* **2004**, *41*, 849−857.
(12) Basbaum, A. I.; Bautista, D. M.; Scherrer, G.; Julius, D. Cellular and molecular mechanisms of pain. *Cell* **2009**, *139*, 267−284.
(13) Kokel, D.; Cheung, C. Y. J.; Mills, R.; Coutinho-Budd, J.; Huang, L.; Setola, V.; Sprague, J.; Jin, S.; Jin, Y. N.; Huang, X.-P.; Bruni, G.; Woolf, C. J.; Roth, B. L.; Hamblin, M. R.; Zylka, M. J.; Milan, D. J.; Peterson, R. T. Photochemical activation of TRPA1 channels in neurons and animals. *Nat. Chem. Biol.* **2013**, *9*, 257−263.
(14) Lam, P.-Y.; Mendu, S. K.; Mills, R. W.; Zheng, B.; Padilla, H.; Milan, D. J.; Desai, B. N.; Peterson, R. T. A high-conductance chemo-optogenetic system based on the vertebrate channel TRPA1b. *Sci. Rep.* **2017**, *7* (1), 11839.
(15) Lam, P.-Y.; Thawani, A. R.; Balderas, E.; White, A. J. P.; Chaudhuri, D.; Fuchter, M. J.; Peterson, R. T. TRPswitch - A step-function chemo-optogenetic ligand for the vertebrate TRPA1 channel. *J. Am. Chem. Soc.* **2020**, *142*, 17457−17468.
(16) Kheradpezhouh, E.; Choy, J. M. C.; Arabzadeh, E.; Daria, V. R. Localized two-photon photoswitching of optovin in rat cortical neurons. *J. Physics D: Appl. Phys.* **2019**, *52*, 254001.
(17) Dollhopf, L. C.; Munos, J. A.; Zheng, K. Y.; Tao, R. X.; Haycock, P. R.; Parsons, P. J.; Peterson, R. T.; Lam, P.-Y.; Fuchter, M. J. Aryl azopyrroles as visible light photoswitchable TRPA1 ligands. *Chem. Sci.* **2025**, *16*, 19777−19785.
(18) Brieke, C.; Rohrbach, F.; Gottschalk, A.; Mayer, G.; Heckel, A. Light-controlled tools. *Angew. Chem., Int. Ed.* **2012**, *51*, 8446−8476.
(19) Zhao, J.; Lin King, J. V.; Paulsen, C. E.; Cheng, Y.; Julius, D. Irritant-evoked activation and calcium modulation of the TRPA1 receptor. *Nature* **2020**, *585*, 141−145.
(20) Ouannes, C.; Wilson, T. Quenching of singlet oxygen by tertiary aliphatic amines. Effect of DABCO (1,4-diazabicyclo[2.2.2]-octane). *J. Am. Chem. Soc.* **1968**, *90*, 6527−6528.
(21) Rodriguez-Serrano, A.; Rai-Constapel, V.; Daza, M. C.; Doerr, M.; Marian, C. M. Internal heavy atom effects in phenothiazinium dyes: enhancement of intersystem crossing via vibronic spin−orbit coupling. *Phys. Chem. Chem. Phys.* **2015**, *17*, 11350−11358.
(22) Mai, S.; Pollum, M.; Martínez-Fernández, L.; Dunn, N.; Marquetand, P.; Corral, I.; Crespo-Hernández, C. E.; González, L. The origin of efficient triplet state population in sulfur-substituted nucleobases. *Nat. Commun.* **2016**, *7* (1), 13077.
(23) Köttner, L.; Wolff, F.; Mayer, P.; Zanin, E.; Dube, H. Rhodanine-based chromophores: Fast access to capable photoswitches and application in light-induced apoptosis. *J. Am. Chem. Soc.* **2024**, *146*, 1894−1903.
(24) Fatima, A.; Chakraborty, P.; Xu, X.; Jones, G. A.; Chambrier, I.; Logan, G.; Cammidge, A. N.; Smith, T.; Hall, C. R.; Meech, S. R. Complex multistate photophysics of a rhodanine photoswitch. *Angew. Chem., Int. Ed.* **2025**, *64* (37), No. e202506137.
(25) Xiao, Y.; Huang, X.; Feng, J.; Ni, Z.; Gai, L.; Xiao, X.; Sui, X.; Lu, H. A simple route toward triplet-forming thionated BODIPY-based photosensitizers. *Dyes Pigm.* **2022**, *200*, 110167.
(26) Tang, J.; Sukhanov, A. A.; Wei, M.; Zhang, X.; Zhao, J.; Dick, B.; Voronkova, V. K.; Li, M. Thionated coumarins: Study of the intersystem crossing and the zero−field splitting of the triplet state using time−resolved transient optical and electron paramagnetic resonance spectroscopies. *Chem.−Eur. J.* **2025**, *31* (21), No. e202404589.

Downloaded from pubs.acs.org/jacsat/article-pdf/doi/10.1021/jacs.6c13271/69052729/jacs.6c13271.pdf by UNIV OF EAST ANGLIA user on 03 November 2026

(27) Fu, Y.; Alachouzos, G.; Simeth, N. A.; Di Donato, M.; Hilbers, M. F.; Buma, W. J.; Szymanski, W.; Feringa, B. L. Establishing PQ-ERA photoclick reactions with unprecedented efficiency by engineering of the nature of the phenanthraquinone triplet state. *Chem. Sci.* **2023**, *14*, 7465−7474.
(28) Lightner, D. A.; Bisacchi, G. S.; Norris, R. D. On the mechanism of the sensitized photooxygenation of pyrroles. *J. Am. Chem. Soc.* **1976**, *98*, 802−807.
(29) Zeinali, N.; Oluwoye, I.; Altarawneh, M.; Dlugogorski, B. Z. The mechanism of electrophilic addition of singlet oxygen to pyrrolic ring. *Theor. Chem. Acc.* **2019**, *138* (7), 90.
(30) Franco, C.; Olmsted, J., III Photochemical determination of the solubility of oxygen in various media. *Talanta* **1990**, *37*, 905−909.
(31) Wilkinson, F.; Abdel-Shafi, A. A. Mechanism of quenching of triplet states by molecular oxygen: Biphenyl derivatives in different solvents. *J. Phys. Chem. A* **1999**, *103*, 5425−5435.
(32) Schweitzer, C.; Mehrdad, Z.; Noll, A.; Grabner, E.-W.; Schmidt, R. Mechanism of photosensitized generation of singlet oxygen during oxygen quenching of triplet states and the general dependence of the rate constants and efficiencies of $O_2(^1_2(^1_2(^3$formation on sensitizer triplet state energy and oxidation potential. *J. Phys. Chem. A* **2003**, *107*, 2192−2198.
(33) Doose, S.; Neuweiler, H.; Sauer, M. A close look at fluorescence quenching of organic dyes by tryptophan. *ChemPhysChem* **2005**, *6*, 2277−2285.
(34) Ley, C.; Morlet-Savary, F.; Jacques, P.; Fouassier, J. Solvent dependence of the intersystem crossing kinetics of thioxanthone. *Chem. Phys.* **2000**, *255*, 335−346.
(35) Taylor, P. R. On the origins of the blue shift of the carbonyl n-π^* transition in hydrogen-bonding solvents. *J. Am. Chem. Soc.* **1982**, *104*, 5248−5249.
(36) Bull, J. N.; Stockett, M. H.; Chakraborty, P.; Ashworth, E. K.; Fatima, A.; Esposito, V. J.; Greetham, G. M.; Malakar, P.; Meech, S. R. Hot ground state cooling following ultrafast photoisomerization: Time-resolved infrared spectroscopy. *J. Phys. Chem. B* **2025**, *129*, 13267−13276.
(37) Fatima, A.; Stockett, M. H.; Ashworth, E. K.; Park, W.; Choi, C.; Wright, J. A.; Chakraborty, P.; Malakar, P.; Meech, S. R.; Bull, J. N. GFP chromophore photophysics: Ultrafast dynamics and hot ground state cooling in the neutral form. *Chem. Sci.* **2026**, *17*, 15098−15107.
(38) Levine, B. G.; Martínez, T. J. Isomerization through conical intersections. *Annu. Rev. Phys. Chem.* **2007**, *58*, 613−634.
(39) Kummer, A. D.; Kompa, C.; Niwa, H.; Hirano, T.; Kojima, S.; Michel-Beyerle, M. E. Viscosity-dependent fluorescence decay of the GFP chromophore in solution due to fast internal conversion. *J. Phys. Chem. B* **2002**, *106*, 7554−7559.
(40) Fatima, A.; Ashworth, E. K.; Chambrier, I.; Cammidge, A. N.; Bressan, G.; Meech, S. R.; Bull, J. N. Ultrafast photophysics of the cyan fluorescent protein chromophore in solution. *Phys. Chem. Chem. Phys.* **2025**, *27*, 9407−9416.
(41) Ashwood, B.; Pollum, M.; Crespo−hernández, C. E. Photochemical and Photodynamical Properties of Sulfur-Substituted Nucleic Acid Bases. *Photochem. Photobiol.* **2018**, *95* (1), 33−58.
(42) Mohamadzade, A.; Ullrich, S. Internal conversion and intersystem crossing dynamics of uracil upon double thionation: a time-resolved photoelectron spectroscopy study in the gas phase. *Phys. Chem. Chem. Phys.* **2020**, *22*, 15608−15615.
(43) Borrego-Varillas, R.; Teles-Ferreira, D. C.; Nenov, A.; Conti, I.; Ganzer, L.; Manzoni, C.; Garavelli, M.; Maria de Paula, A.; Cerullo, G. Observation of the sub-100 fs population of a dark state in a thiobase mediating intersystem crossing. *J. Am. Chem. Soc.* **2018**, *140*, 16087−16093.
(44) Glover, H.; Saßmannshausen, T.; Bertrand, Q.; Trabuco, M.; Slavov, C.; Bacchin, A.; Andres, F.; Kondo, Y.; Stipp, R.; Wranik, M.; et al. Photoswitch dissociation from a G protein-coupled receptor resolved by time-resolved serial crystallography. *Nat. Commun.* **2024**, *15* (1), 10837.
(45) Meech, S. R. Excited state reactions in fluorescent proteins. *Chem. Soc. Rev.* **2009**, *38*, 2922.
(46) Carrascosa, E.; Bull, J. N.; Scholz, M. S.; Coughlan, N. J. A.; Olsen, S.; Wille, U.; Bieske, E. J. Reversible photoisomerization of the isolated green fluorescent protein chromophore. *J. Phys. Chem. Lett.* **2018**, *9*, 2647−2651.
(47) Niwa, H.; Inouye, S.; Hirano, T.; Matsuno, T.; Kojima, S.; Kubota, M.; Ohashi, M.; Tsuji, F. Chemical nature of the light emitter of the Aequorea green fluorescent protein. *Proc. Nat. Acad. Sci. U. S. A.* **1996**, *93*, 13617−13622.
(48) Follenius-Wund, A.; Bourotte, M.; Schmitt, M.; Iyice, F.; Lami, H.; Bourguignon, J.-J.; Haiech, J.; Pigault, C. Fluorescent derivatives of the GFP chromophore give a new insight into the GFP fluorescence process. *Biophys. J.* **2003**, *85*, 1839−1850.
(49) Voskresenska, V.; Wilson, R. M.; Panov, M.; Tarnovsky, A. N.; Krause, J. A.; Vyas, S.; Winter, A. H.; Hadad, C. M. Photoaffinity labeling via nitrenium ion chemistry: Protonation of the nitrene derived from 4-amino-3-nitrophenyl azide to afford reactive nitrenium ion pairs. *J. Am. Chem. Soc.* **2009**, *131*, 11535−11547.
(50) Smith, E.; Collins, I. Photoaffinity labeling in target- and binding-site identification. *Future Med. Chem.* **2015**, *7*, 159−183.
(51) Ge, S.-S.; Chen, B.; Wu, Y.-Y.; Long, Q.-S.; Zhao, Y.-L.; Wang, P.-Y.; Yang, S. Current advances of carbene-mediated photoaffinity labeling in medicinal chemistry. *RSC Adv.* **2018**, *8*, 29428−29454.
(52) Choi, H.; Kim, M.; Jang, J.; Hong, S. Visible−light−induced cysteine−specific bioconjugation: Biocompatible thiol-ene click chemistry. *Angew. Chem., Int. Ed.* **2020**, *59*, 22514−22522.
(53) Wan, C.; Hou, Z.; Yang, D.; Zhou, Z.; Xu, H.; Wang, Y.; Dai, C.; Liang, M.; Meng, J.; Chen, J.; Yin, F.; Wang, R.; Li, Z. The thiol-sulfoxonium ylide photo-click reaction for bioconjugation. *Chem. Sci.* **2023**, *14*, 604−612.
(54) Campaniço, A.; Baran, M.; Bowie, A. G.; Longley, D. B.; Harrison, T.; McGouran, J. F. Chemical- and photo-activation of protein-protein thiol-ene coupling for protein profiling. *Commun. Chem.* **2025**, *8* (1), 25.
(55) Velema, W. A.; Szymanski, W.; Feringa, B. L. Photopharmacology: Beyond proof of principle. *J. Am. Chem. Soc.* **2014**, *136*, 2178−2191.
(56) Hüll, K.; Morstein, J.; Trauner, D. *In vivo* photopharmacology. *Chem. Rev.* **2018**, *118*, 10710−10747.
(57) Lerch, M. M.; Hansen, M. J.; van Dam, G. M.; Szymanski, W.; Feringa, B. L. Emerging targets in photopharmacology. *Angew. Chem., Int. Ed.* **2016**, *55*, 10978−10999.
(58) Dang, T.; Zhang, Z.-Y.; Li, T. Visible-light-activated heteroaryl azoswitches: Toward a more colorful future. *J. Am. Chem. Soc.* **2024**, *146*, 19609−19620.
(59) Wang, L.; Wu, Y.; Tan, X.; Xia, C. Visible and near-infrared photopharmacology: Wavelength-redshift strategies for spatiotemporally precise therapeutics. *J. Med. Chem.* **2026**, *69*, 1878−1915.
(60) Naimovicius, L.; Miroshnichenko, M.; Opar, E.; Hölzel, H.; Morikawa, M.-A.; Kimizuka, N.; Dapkevicius, M.; Lekavičius, J.; Radiunas, E.; Kazlauskas, K.; et al. Noninvasive cardiac modulation via triplet-sensitized photoswitching in the phototherapeutic window. *Nat. Commun.* **2025**, *16* (1), 6377.

Downloaded from pubs.acs.org/jacsat/article-pdf/doi/10.1021/jacs.6c13271/69052729/jacs.6c13271.pdf by UNIV OF EAST ANGLIA user on 03 November 2026

https://doi.org/10.1021/jacs.6c13271
J. Am. Chem. Soc. XXXX, XXX, XXX−XXX